Competitive Intramolecular Aryl- and Alkyl-C–H Bond Activation and Ligand Evaporation from Gaseous Bisimino Complexes $[Pt(L)(CH_3)((CH_3)_2S)]^+$ ($L = C_6H_5N{=}C(CH_3){-}C(CH_3){=}NC_6H_5$)

by **Burkhard Butschke**[a]), **Maria Schlangen**[a]), **Detlef Schröder**[b]), and **Helmut Schwarz***[a])

[a]) Institut für Chemie, Technische Universität Berlin, Straße des 17. Juni 135, D-10623 Berlin (fax: +49 30-314-21102; e-mail: Helmut.Schwarz@mail.chem.tu-berlin.de)

[b]) Institute of Organic Chemistry and Biochemistry, Flemingovo nám. 2, CZ-16610 Prague 6

Mechanistic details for the formation of methane from the title compound as well as the combined elimination of $(CH_3)_2S/CH_4$ are derived from various mass-spectrometric experiments including deuterium-labeling studies and DFT calculations. For the first process, *i.e.*, methane formation, we have identified three competing pathways in which the intact, Pt-bonded methyl group combines with a H-atom that originates from a phenyl substituent (*ca.* 7%), the dimethyl sulfide ligand (*ca.* 41%), and a methyl group of the diazabutadiene backbone (*ca.* 52%). In contrast, in the combined $(CH_3)_2S/CH_4$ elimination, the methane is specifically formed from the Pt-bound CH_3 group and a H-atom provided by one of the phenyl groups ('cyclometalation').

Introduction. – Ever since the introduction of the seminal *Shilov* system [1], platinum has served as a particularly promising metal for the activation and functionalization of saturated hydrocarbons, including methane, at ambient conditions, even though the current laboratory procedures are still far from being useful for practical applications in large-scale processes [2]. While solution-phase experiments have provided a wealth of knowledge about various aspects relevant in the context of activation of C–H bonds by transition-metal complexes [3], gas-phase studies, combined with computational investigations, can provide insight complementary to these more traditional approaches in revealing the details of the elementary steps involved in the bond activation, as well as the role of the intrinsic electronic structures of the transition-metal site [4]. Notwithstanding the advantages and also not questioning the inherent merits of either approach, there is occasionally a debate about the relevance of gas-phase studies for describing reactions occurring in condensed phase media [5], as, for example, the activation of benzene by cationic $[Pt(L)(CH_3)]^+$ complexes [6], where L corresponds to a bidentate nitrogen ligand[1]). Of quite some mechanistic interest in this context are intramolecular C–H-bond activation reactions, *e.g.*, *ortho*-metalations of phenyl ligands [8][2]).

In this communication, we describe some intriguing aspects of the gas-phase behavior of the cationic complex $[Pt(L)(CH_3)((CH_3)_2S)]^+$ with $L = C_6H_5N{=}$

[1]) For the thermal gas-phase reactions of these complexes with methane, see [7].

[2]) For other examples of intramolecular 'suicidal' oxidations of chelating ligands by the transition-metal core, see [9] and [10].

$C(CH_3)-C(CH_3)=NC_6H_5$ (**1**); this complex and its deuterated analogues [D_6]-**1**, [D_{10}]-**1**, and [D_{16}]-**1** are generated directly from methanolic solutions of dimeric $[Pt(CH_3)_2(\mu\text{-}(CH_3)_2S)]_2$ and the corresponding ligands by means of electrospray ionization (ESI) [11], and are probed by mass-spectrometric methods.

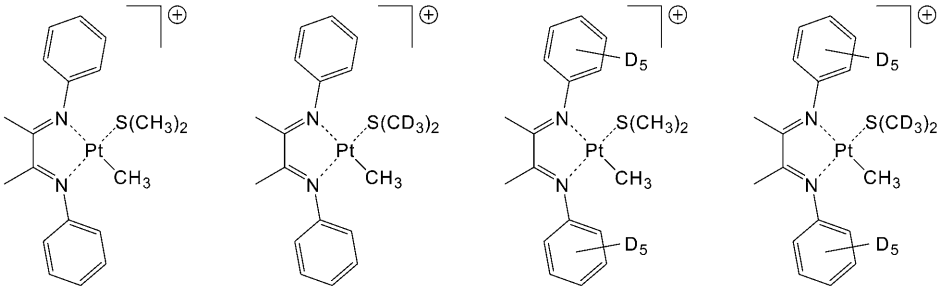

Experimental and Computational Details. – The present experiments were performed with a *VG BIO-Q* mass spectrometer of QHQ configuration (Q: quadrupole, H: hexapole) equipped with an ESI source as described in detail in [12]. In brief, millimolar solutions of dimeric $[Pt(CH_3)_2(\mu\text{-}(CH_3)_2S)]_2$ and the desired ligand $C_6H_5N=C(CH_3)-C(CH_3)=NC_6H_5$ in pure CH_3OH were introduced through a fused-silica capillary to the ESI source *via* a syringe pump (*ca.* 3 µl/min). For the generation of complexes with $(CD_3)_2S$ as a ligand (instead of $(CH_3)_2S$), an excess of $(CD_3)_2S$ was added to the soln. N_2 was used as a nebulizing and drying gas at a source temp. of 80°. Maximal yields of the derived $[Pt(L)(CH_3)((CH_3)_2S)]^+$ complex were achieved by adjusting the cone voltage around 60 V. The identity of the ions was confirmed by comparison with the expected isotope patterns [13] and collision-induced dissociation (CID) experiments. The isotope pattern also assisted in the choice of the adequate precursor ion in order to avoid coincidental mass overlaps of isobaric species in the mass-selected ion beam [14]. For CID experiments, the ions of interest were mass-selected using Q1, interacted with Xe as a collision gas (typically $p = 10^{-4}$ mbar) at variable collision energies of $E_{lab} = 0-20$ eV, while scanning Q2 to monitor the ionic products. Parent-ion scans, in which the first analyzer scans a regular mass spectrum while the second mass analyzer is fixed to the *m/z* value of the desired product ion, were used to identify all ions ('parents'), which give rise to a particular product ion.

In the computational studies, which only aim at a *qualitative* description of the unimolecular reactions of $[Pt(L)(CH_3)((CH_3)_2S)]^+$, the geometries of all species were optimized at the B3LYP level of theory [15] as implemented in the Gaussian03 program package [16] using basis sets of approximately triple-ξ quality. For H-, C-, N-, and S-atoms, these were the triple-ξ plus polarization basis sets (TZVP) of *Ahlrichs* and co-workers [17]. For Pt, the Stuttgart-Dresden scalar relativistic pseudopotential (ECP60MDF replacing 60 core electrons) was employed in conjunction with the corresponding (8s,7p,6d)/[6s,5p,3d] basis set describing the 6s5d valence shell of Pt[3]). The nature of the stationary structures as minima or saddle points was characterized by frequency analysis, and intrinsic reaction coordinate (IRC) calculations were performed to link the transition structures with the respective intermediates [19]. Energies (given in kJ mol^{-1}) are corrected for (unscaled) zero-point vibrational energy contributions. The discussion will be confined to the singlet states of the various ions, as triplet states, based on exploratory calculations, are in general much higher in energy for all species investigated.

Results and Discussion. – Under soft conditions of ionization, ESI of a methanolic solution of $[Pt(CH_3)_2(\mu\text{-}(CH_3)_2S)]_2$ and $C_6H_5N=C(CH_3)-C(CH_3)=NC_6H_5$ affords the

[3]) The basis set and ECP correspond to the revision from June 27, 1997, of the Stuttgart/Dresden groups; also see [18].

title compound **1**, while fragmentations start to occur upon gradually enforced ionization conditions [12][20][21]. The relative abundances of **1** and its primary fragments in the ion source-spectra are given in *Table 1*. One primary fragment corresponds to the loss of methane, [**1** – CH_4], and the second to a combined elimination of dimethyl sulfide and methane, [**1** – $(CH_3)_2S/CH_4$]. Even at the detection limit of the mass spectrometer, we do not observe a fragment ion that corresponds to the loss of only $(CH_3)_2S$, *i.e.*, [**1** – $(CH_3)_2S$], although such a species is formed using other ligands L, as for example 2,2′-bipyridine or 1,10-phenanthroline [7]. As expected, the extent of fragmentation increases with increasing the cone voltage (U_c) which determines the amount of energizing collisions occurring in the source region [12][20][21]. At the lowest cone voltage applied, CH_4 loss is favored over the combined elimination of $(CH_3)_2S/CH_4$; however, the latter gains in importance upon increasing U_c. We also note clustering of the fragment ions with N_2, the amount of which is heavily affected by the experimental conditions chosen.

Table 1. *Relative Abundances of* **1** *and Its Primary Fragment Ions [***1** *– CH_4] and [***1** *– $(CH_3)_2S/CH_4$] in the ESI-Source Mass Spectra of a Dilute Methanolic Solution of [$Pt(CH_3)_2(\mu\text{-}(CH_3)_2S)]_2$ and $C_6H_5N{=}C(CH_3){-}C(CH_3){=}NC_6H_5$ at Different Cone Voltages,* U_c[a])[b])

	$U_c = 40$ V	$U_c = 50$ V	$U_c = 60$ V
1	100	100	100
[**1** – CH_4]	16	64	192
[**1** – $(CH_3)_2S/CH_4$]	9	71	450

[a]) Intensities are given in % relative to the precursor ion **1** with the Pt isotope ^{196}Pt. [b]) In addition to the signals shown in the table, one observes clusters of fragment ions with the nebulizing gas N_2. Not even at the detection limit, a signal corresponding to the exclusive loss of $(CH_3)_2S$ is observed (see text).

Further information on the genesis of the two product ions is produced by subjecting mass-selected **1** to a CID experiment as well as the product ions to parent-ion scans. In the former, we observe once more the eliminations of CH_4 and of $(CH_3)_2S/CH_4$, while no signal for an exclusive loss of $(CH_3)_2S$ from **1** is observed. As shown in *Fig. 1*, the major primary products obtained upon CID of mass-selected **1** correspond to the fragments [**1** – CH_4] and [**1** – $(CH_3)_2S/CH_4$], which are already observed upon ESI at enforced conditions. In addition to these major fragments, a small signal which formally is due to [**1** – C_3H_8] is observed (see inset in *Fig. 1*), which indicates the occurrence of C–C-bond coupling reactions to a very small extent. The threshold behavior of **1** is of composite nature, and a phenomenological modeling of the breakdown graph using sigmoid functions [22][4]) reveals the competition of CH_4 and $(CH_3)_2S/CH_4$ eliminations at low collision energies with another component, most likely a direct fragmentation pathway becoming predominant at a collision energy of *ca.* 4 eV. At higher collision energies, several consecutive dissociation reactions take place of which we only mention the formation of an ion with m/z 118, most probably the nitrilium cation $[C_6H_5{-}N{\equiv}C{-}CH_3]^+$, which is a major fragment at elevated collision energies.

4) For several applications of this fitting method to transition-metal ions, see [10] and [23].

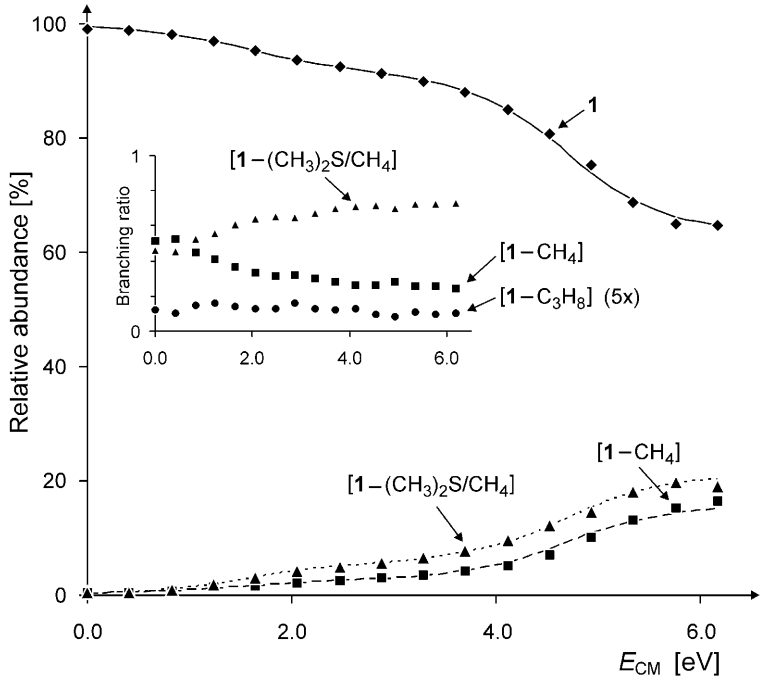

Fig. 1. *Breakdown graph for the CID of mass-selected* **1** (*m*/*z* 507) *showing the abundances of the parent ion* **1** (◆) *and the primary fragments [***1** *– CH_4]* (*m*/*z* 491; ■) *and [***1** *– $(CH_3)_2S/CH_4$]* (*m*/*z* 429; ▲) *as a function of the collision energy in the center-of-mass frame.* Note that, at high collision energies, the consecutive fragmentations observed are summed into the primary dissociation products. The inset shows the branching ratios of the two major channels to *m*/*z* 491 (■) and 429 (▲), as well as the minor fragment [**1** – C_3H_8] (*m*/*z* 463; ●) described in the text. The lines connecting the data points represent the results of the fit of the ion profiles using sigmoid functions (see text).

What remains unclear, however, is the mechanism of the combined $(CH_3)_2S/CH_4$ elimination about which the CID spectra do not provide further information, as neither [**1** – $(CH_3)_2S$] is observed, nor does the abundance of [**1** – CH_4] cross-correlate with that of [**1** – $(CH_3)_2S/CH_4$], as expected for a sequential elimination of first CH_4 and then $(CH_3)_2S$. A clue to the possible precursor(s) of the $(CH_3)_2S/CH_4$-elimination product ion is provided by a parent-ion scan, which reveals only **1** but not [**1** – CH_4] or [**1** – $(CH_3)_2S$] as a precursor, which suggests the reaction sequence depicted in *Scheme 1*[5]).

Most revealing in this context are CID experiments conducted with the labeled ions $[D_6]$-**1** and $[D_{10}]$-**1**. For the former isotopologue, methane loss corresponds to the

---

[5]) While we cannot strictly rule out the intermediacy of short-lived [**1** – $(CH_3)_2S$] ions, *i.e.*, a sequential process with $k_4 \ll k_5$, the experimental data clearly demonstrate that k_2 must be too small to contribute to the formation of [**1** – $(CH_3)_2S/CH_4$], because [**1** – CH_4] can clearly be found in the source spectrum under the conditions chosen for the parent-ion scan, which does not hold true for [**1** – $(CH_3)_2S$]. Unfortunately, the presently available set of data does not permit to quantify any k_i. For a related situation, *i.e.*, the sequential reaction $Pd^+ + CH_3I \xrightarrow{k_1} Pd(CH_3)^+ + I^\cdot$, $Pd(CH_3)^+ + CH_3I \xrightarrow{k_2} Pd(CH_2I)^+ + CH_4$, with $k_1 \ll k_2$, see [24].

Scheme 1

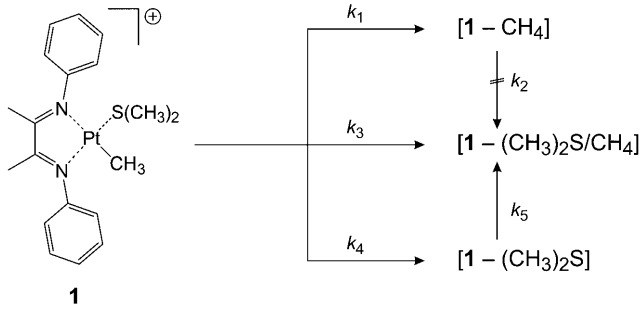

elimination of CH_4 and CH_3D ($\Delta m = 16$ and 17 in a ratio of *ca.* 2:1), and, for the combined dimethyl sulfide/methane channel, one observes only one signal with $\Delta m = 84$, corresponding to $(CD_3)_2S/CH_4$. In contrast, in the CID spectrum of $[D_{10}]$-**1**, the corresponding mass differences amount to $\Delta m = 16$ (CH_4 loss) and $\Delta m = 79$ (combined eliminations of $(CH_3)_2S$ and CH_3D). These findings demonstrate unequivocally that the two competitive channels are not linked to each other such that the cation [**1** – CH_4] serves as a precursor for the formation of [**1** – $(CH_3)_2S/CH_4$]. The latter product ion is, as suggested in *Scheme 1*, either formed directly from **1** or from a very short-lived intermediate [**1** – $(CH_3)_2S$][6]). Ion-source spectra, recorded at different cone voltages, give, by and large, the same results except that, in the formation of methane, a H-atom from the phenyl group is incorporated to *ca.* 7% (*Table 2*).

Table 2. *Branching Ratios* (in %) *for the Fragments due to Loss of Methane in the Ion-Source Mass Spectra of the [D_6]-***1**, *[D_{10}]-***1**, *and [D_{16}]-***1** *Isotopologues Derived from the [$Pt(CH_3)_2(\mu\text{-}(CH_3)_2S)]_2$/$C_6H_5N{=}C(CH_3){-}C(CH_3){=}NC_6H_5$ System Taken at Different Cone Voltages.* The numbers result from modeling of the corresponding isotope patterns using a linear combination of the single isotope patterns.

Losses of	[D_6]-**1**			[D_{10}]-**1**			[D_{16}]-**1**		
	50 V	60 V	70 V	50 V	60 V	70 V	50 V	60 V	70 V
CH_4	59	63	65	94	93	93	52	57	60
CH_3D	41	37	35	6	7	7	48	43	40

Further, our data imply that *i*) the evaporation of the $(CH_3)_2S$ ligand is not preceded by H/D scrambling involving the dimethyl sulfide group and *ii*) the formation of methane proceeds competitively *via* several distinct channels. A simplified mechanism for the latter reaction that does not take into account the small contribution of a phenyl group is suggested in *Scheme 2*. The justification for excluding $(CH_3)S$ loss from **4a** or **4c** is based on the parent-ion spectra and supported by computational investigations (see *Fig. 2*, below).

For CH_4 loss from **1**, three pathways compete to serve as a source for the fourth H-atom; while the contribution of the phenyl group is rather small (*ca.* 7%) that of a CH_3

[6]) For other examples of the rare case of rapid consecutive eliminations of two different neutral molecules, see [25].

Scheme 2

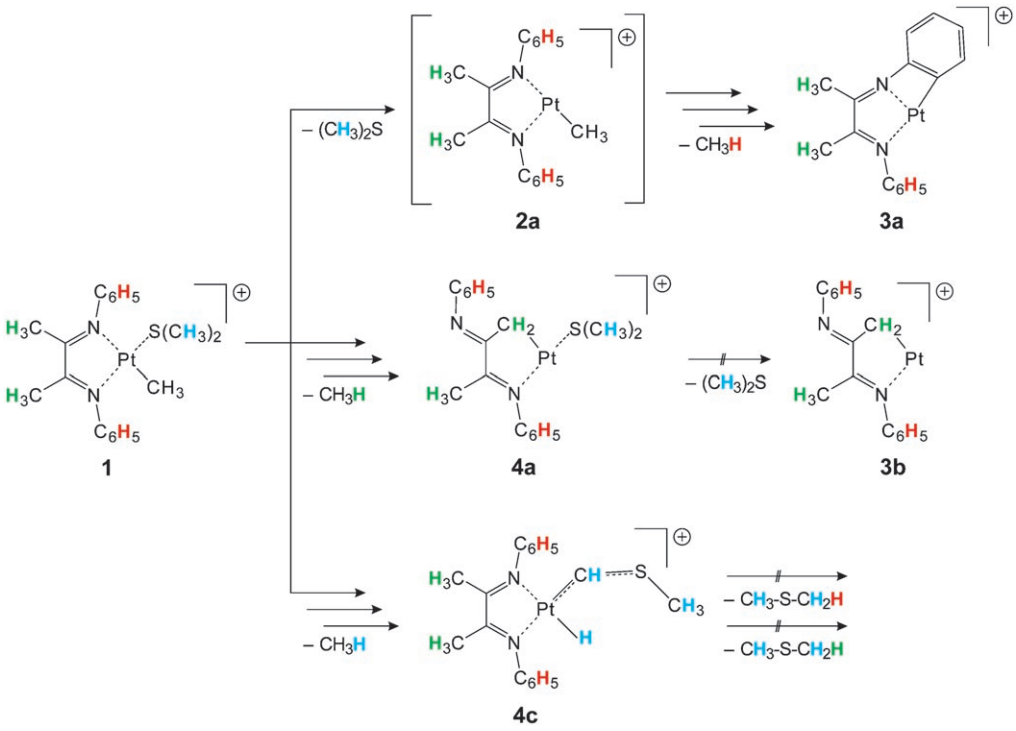

group of the $(CH_3)_2S$ ligand (*ca.* 41%) and a CH_3 group of the diazabutadiene backbone (*ca.* 52%) are comparable. In this assignment, possible kinetic isotope effects are ignored, because the data in *Table 2* indicate an only small dependence of the isotope distributions on the cone voltages applied.

In distinct contrast, for the combined $(CH_3)_2S/CH_4$-loss channel after elimination of the intact $(CH_3)_2S$ group, in the actual CH_4-formation step from the short-lived intermediate [**1** – $(CH_3)_2S$] (**2a**), it is specifically a H-atom from one of the phenyl rings that, together with the CH_3 group bound to the Pt-center, is released as CH_4. Thus, one encounters the rather rare situation of a competitive, intramolecular C–H-bond activation of an alkyl–H *vs.* aryl–H bond[7]).

We have also attempted to obtain further insight in mechanistic aspects of the reactions depicted in *Scheme 2* by means of complementary DFT calculations; in the calculations, we have not included the minor path of the CH_4-loss channel (*ca.* 7%) involving phenyl–H bond activation. Being aware of the problems one occasionally encounters in describing transition-metal mediated reactions by DFT-based methods [27], we did not aim at a quantitative correlation of the computational results with the experimental findings; rather, *qualitative* aspects deemed us more important. In *Fig. 2*, the most pertinent data are summarized.

---

[7]) For a related case where the C–H-activation process is preceded by ligand loss, see [26].

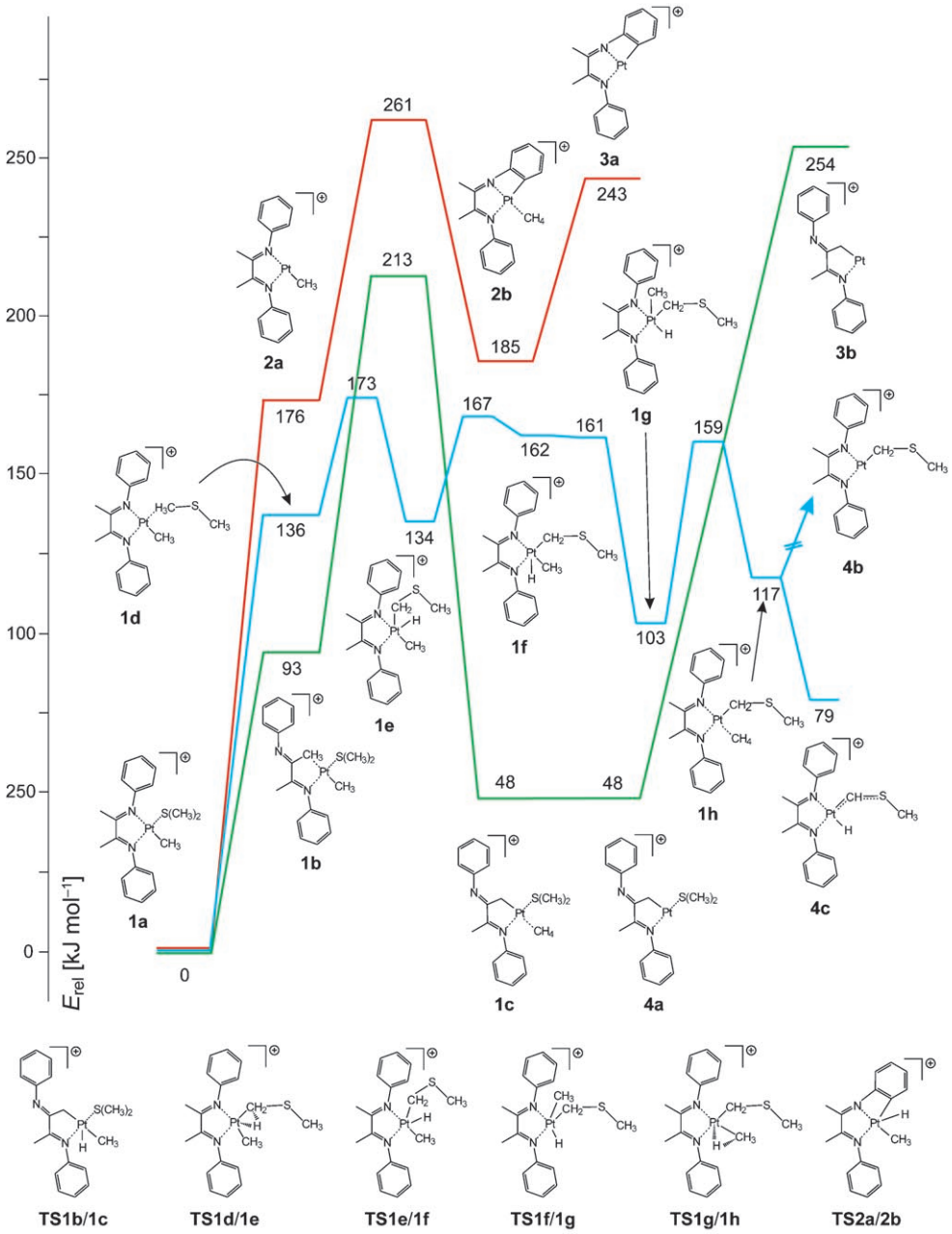

Fig. 2. *Computed potential-energy profile for the competing eliminations of CH_4 and $(CH_3)_2S$ as well as the combined loss* via *initial C−H-bond activation of a methyl group of the bisimino ligand* (green pathway), *initial loss of dimethyl sulfide* (red pathway), *and initial C−H-bond activation of a methyl group of the dimethyl sulfido ligand* (blue pathway). We note that, for various species given in *Fig. 2*, several conformers of comparable energies have been located. As to the notations used, different letters describe isomers, *e.g.*, **1a** and **1b**, whereas different numbers are used to distinguish between various elemental compositions, *e.g.*, **1a** and **2a**. Further, one cannot rule out the possibility of an as yet unknown path that has escaped our rather extensive DFT screening of the potential-energy surface.

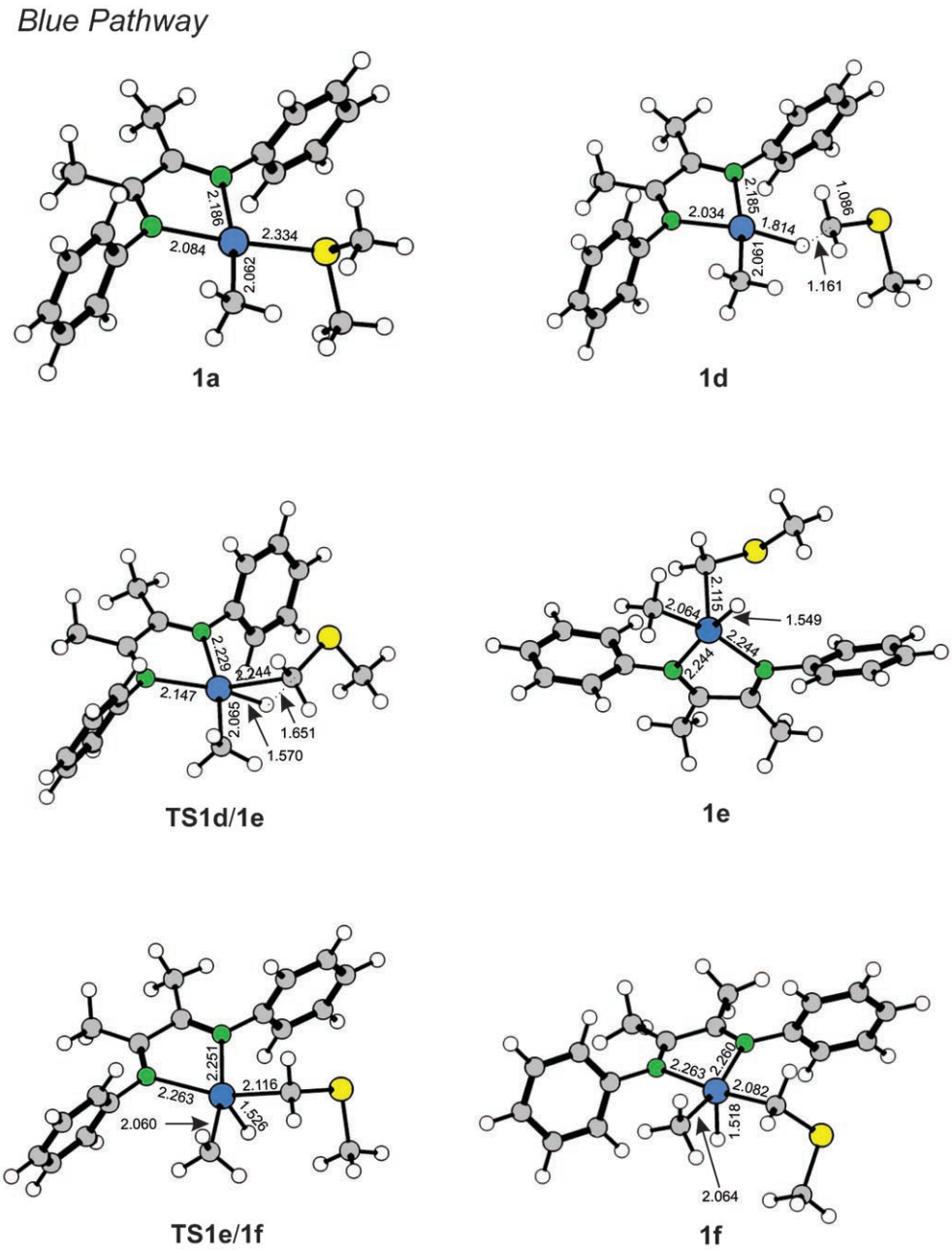

Fig. 3. *Geometry-optimized structures of the species mentioned in* Fig. 2 *together with the relevant bond lengths* (*r* in Å) *around the Pt core.* For the description of the *Pathways*, see the legend to *Fig. 2*.

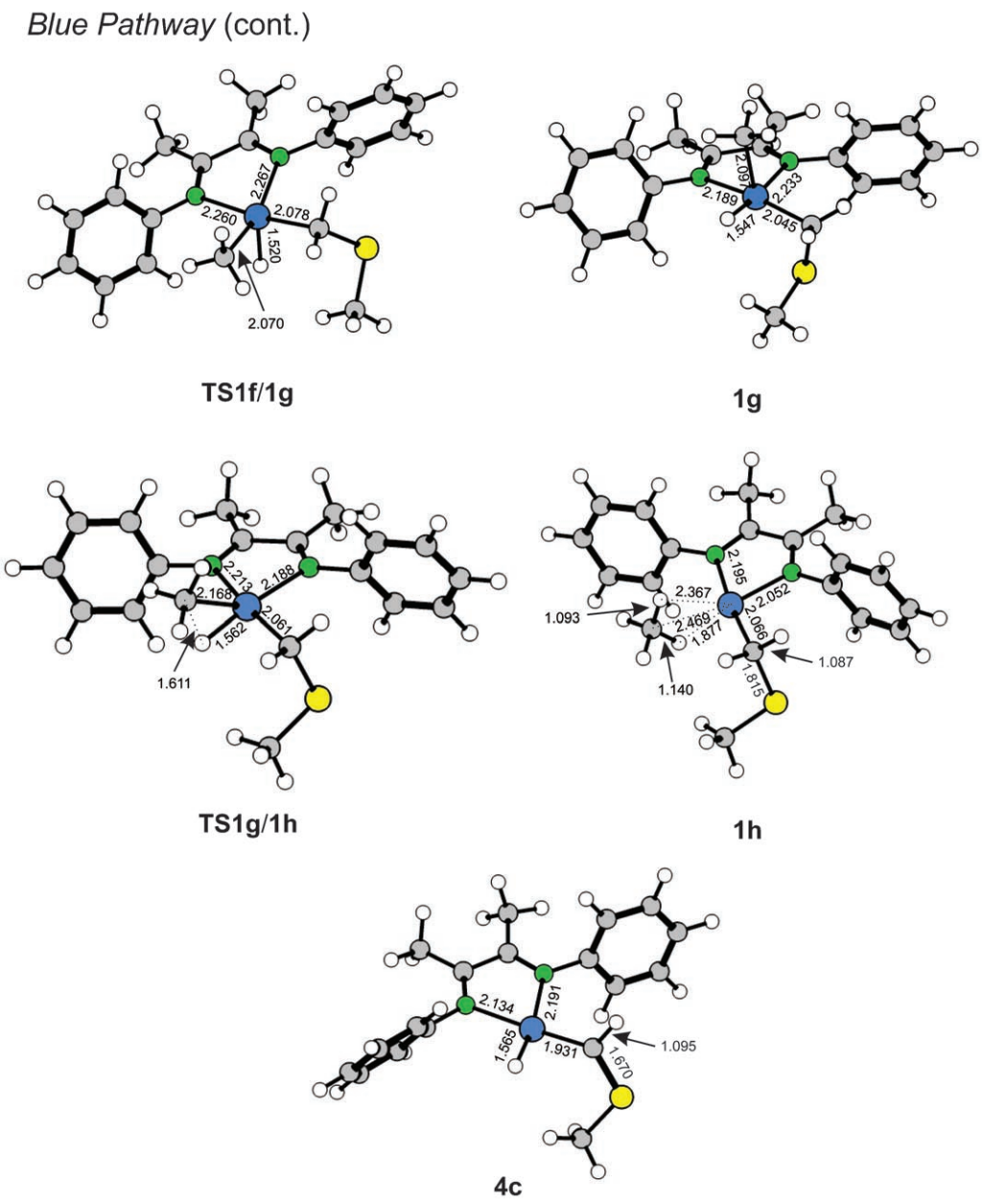
Blue Pathway (cont.)
2.267
2.260
2.078
1.520
2.070
TS1f/1g
2.189
2.233
1.547
2.045
1g
2.213
2.188
2.168
2.061
1.562
1.611
TS1g/1h
2.195
2.367
2.052
1.093
2.469
1.877
2.066
1.087
1.140
1.815
1h
2.134
2.191
1.565
1.931
1.095
1.670
4c

Fig. 3 (cont.)

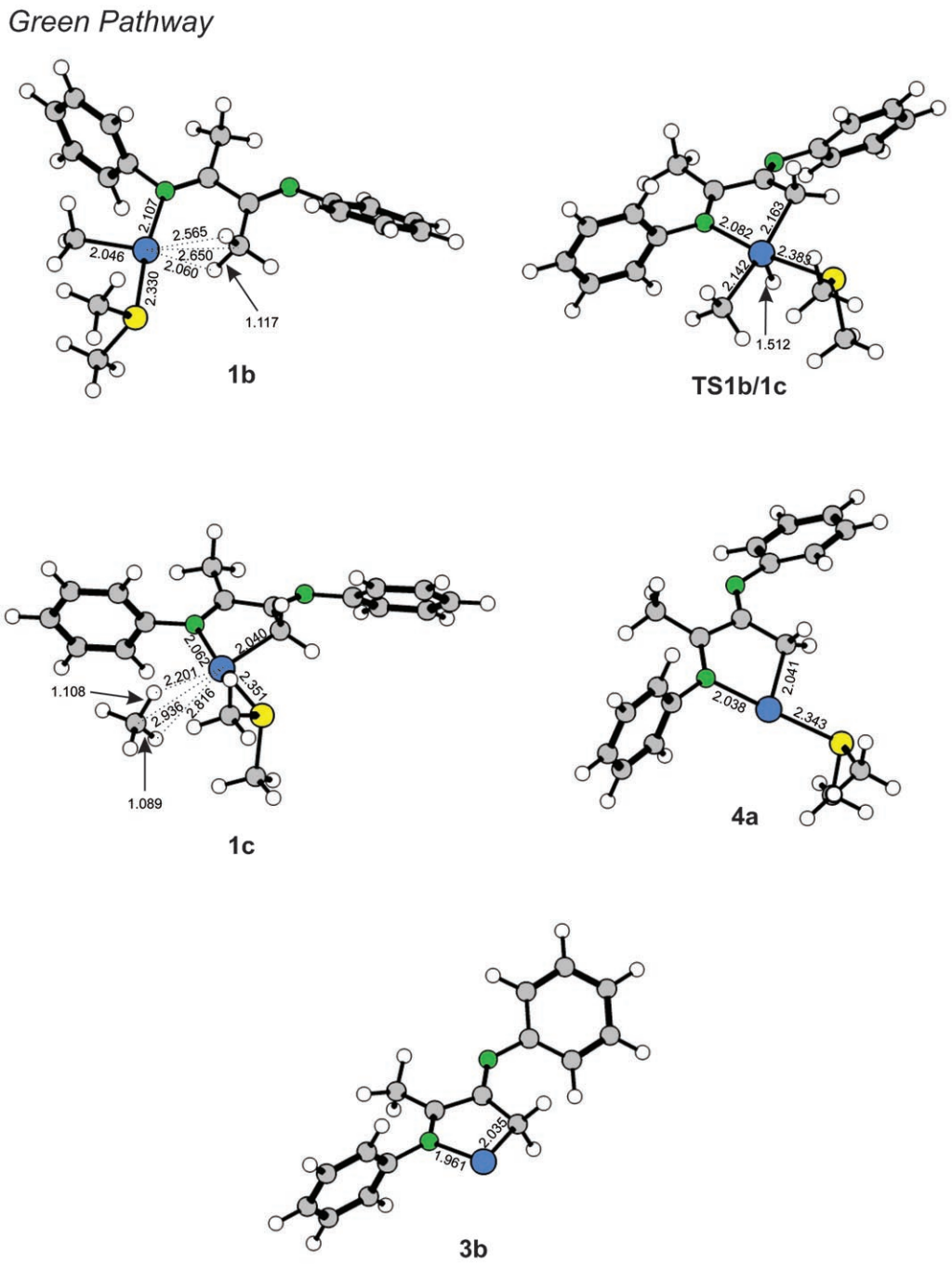
Green Pathway
2.107
2.046
2.330
2.565
2.650
2.060
1.117
1b
2.082
2.163
2.383
2.142
1.512
TS1b/1c
2.062
2.040
2.201
1.108
2.936
2.816
2.351
1.089
1c
2.038
2.041
2.343
4a
2.035
1.961
3b

Fig. 3 (cont.)

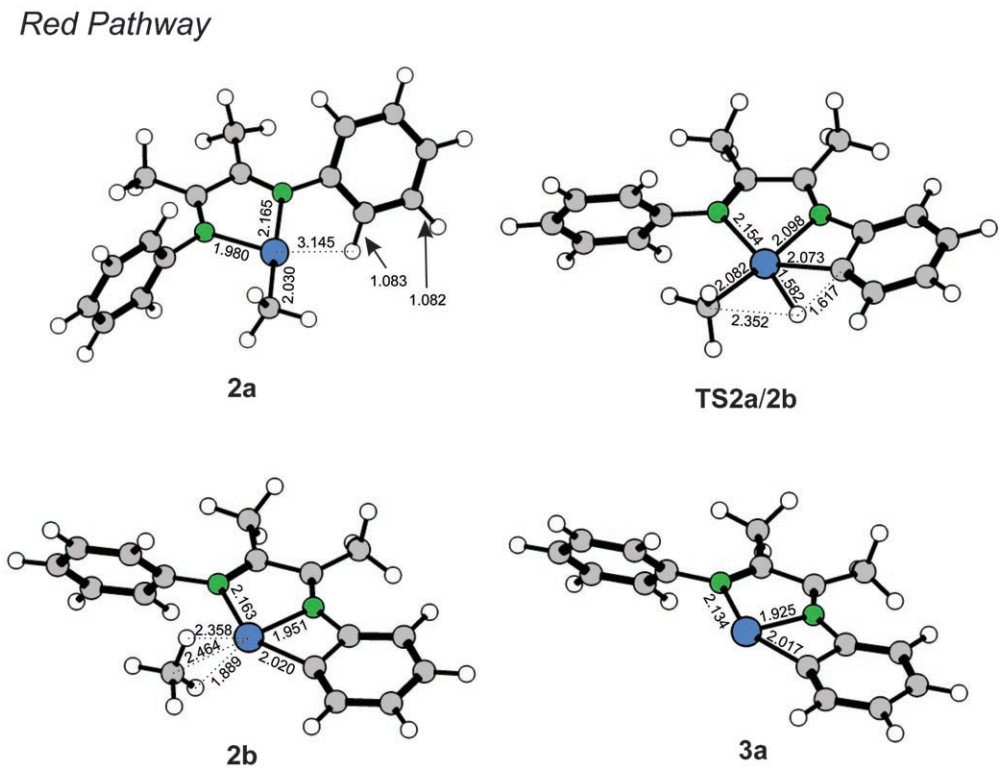

Fig. 3 (cont.)

With regard to the loss of CH_4 from **1**, the DFT calculations (*Fig. 2*) demonstrate the existence of two distinct pathways whose energy demands are comparable. In the first variant, after decomplexation of one imino ligand upon increasing the internal energy content in CID (**1a** → **1b**), C−H-bond activation of the C−CH_3 group, presumably *via* a metathesis-like mechanism[8]), leads to complex **1c**, which is eventually converted to the products **4a** and CH_4. In the second route, the Pt-core retains its chelating interaction with both N-atoms of the ligand, and the reaction commences with activation of a C−H bond of the reoriented $(CH_3)_2S$ group (**1a** → **1d** → **1e** → **1f** → **1g** → **1h**)[9]). Complex **1h** has then two potential options for the liberation of CH_4. However, for the first one, an uphill process, the resulting ion **4b** could not be located computationally; rather, loss of CH_4 from **1h** is accompanied by a further C−H-bond activation step (**1h** → **4c**). Common to the CH_4-loss channels are

---

[8]) For a recent, systematic study of mechanistic variants of gas phase, metal-mediated C−H-bond activation, see [4f].

[9]) We have also located a transition structure for the *direct* path **1e** → **1h** with a relative energy of 210 kJ mol^{-1}, which is much too high in energy to compete with the sequence **1e** → **1f** → **1g** → **1h**. For the very first step, *i.e.*, the reorientation of the $(CH_3)_2S$ group (**1a** → **1d**), all attempts failed to locate a transition structure. The same holds true for the location of **TS 1a/1b**.

three features: *i*) The rate-limiting step is always associated with activation of a C–H bond; *ii*) the formal oxidation state of Pt is conserved in the course of the reaction in that one starts from Pt^{II} (in **1a**) and the product ion **4a** corresponds to Pt^{II}, although the intermediates **1e**, **1f**, and **1g**, as well as the carbene complex **4c** formally correspond to Pt^{IV}, and *iii*) further decompositions of either [**1** – CH_4] product ions *via* elimination of $(CH_3)_2S$ to generate [**1** – $(CH_3)_2S/CH_4$], *e.g.*, **3a** or **3b**, are rather energy-demanding, thus explaining why this reaction is not observed experimentally. Finally, according to the DFT data, CH_4 loss is overall energetically less-demanding than the combined $(CH_3)_2S/CH_4$-elimination channel.

As to the latter, based on DFT we identified a pathway (**1a** → **2a** → **2b** → **3a**), which is in keeping with the labeling data. However, the fact that the transition structure **TS2a/2b** associated with the rate-limiting C–H-bond activation step (**2a** → **2b**) is located well above the cyclometalation product ion **3a**, as well as higher in energy than the initially formed intermediate **2a**, cannot explain the experimental finding that a signal for the ion **2a** is not observed experimentally. Quite likely, either more elaborate computations are needed to describe the transformation **2a** → **2b** more accurately, or the neglect of the direct C–H-bond activation in the CH_4-loss channel is not justfied as it may be followed by a rapid loss of $(CH_3)_2S$. Last but not least, the seemingly negligible formal loss of C_3H_8 from the parent ion might yet even provide another route to the fragment **3a**, in that not $(CH_3)_2S + CH_4$ ($\Sigma\Delta_f H = -112$ kJ mol^{-1}), but instead $C_3H_8 + H_2S$ ($\Sigma\Delta_f H = -125$ kJ mol^{-1}) are formed as thermodynamically even slightly more favored neutral products. However, the intensity profile of [**1** – C_3H_8] in *Fig. 1*, the generally small abundance of this fragment, as well as the extensive H/D equilibration in the propane-loss channel for [D_6]-**1** render unlikely this scenario.

Fig. 3 shows the geometry-optimized structures of the species mentioned in *Fig. 2* together with the relevant bond lengths (*r* in Å) around the Pt-core. Of the vast amount of structural details in *Fig. 3*, only a few key features are discussed. The precursor species **1a** bears a quasi-square-planar coordination geometry with r_{Pt-C} and $r_{Pt-N,cis}$ of *ca.* 2.1 Å, whereas the bond length to the N-atom *trans* to the CH_3 group ($r_{Pt-N,trans}$) is *ca.* 0.1 Å larger, and the Pt–S distance amounts to *ca.* 2.3 Å. Except for r_{Pt-S}, these features do not change upon partial decomplexation of the $(CH_3)_2S$ ligand (**1a** → **1d**), whereas the oxidative addition *via* **TS1d/1e** to yield the formal Pt^{IV} compound **1e** is associated with a change to a roughly square-pyramidal geometry concomitant with a significant increase of both r_{Pt-N} bonds to 2.244 Å, which remains similar upon interchanges of the CH_3, CH_3SCH_2, and H ligands (**1e** → **1f** → **1g**). Upon reductive elimination of CH_4 *via* **TS1g/1h**, however, the resulting formal Pt^{II} species again bears significantly shorter Pt–N bonds, quite similar to those in **1a**. Interestingly, loss of CH_4 from the coordination complex **1g** does not lead to the Pt^{II} species **4b**, but instead to a spontaneous C–H-bond insertion to afford the Pt^{IV} carbene **4c** with again enlarged Pt–N distances. The alternative mechanism *via* activation of a C–H bond of one of the CH_3 groups of the bisimino ligand commences with the cleavage of one of the Pt–N bonds (**1a** → **1b**) while not largely affecting the remaining r_{Pt-C}, $r_{Pt-N,cis}$, and r_{Pt-S}. The same holds true for the following C–H-bond activation (**1b** → **TS1b/1c** → **1c**), except that the Pt–C bond in **1c** now involves the CH_3 C-atom of the bisimino ligand, rather than the original CH_3 ligand ($r_{Pt-C} = 2.040$ Å in **1c** compared to 2.062 Å in **1a**). Loss of CH_4 from **1c** hardly affects the structure of the resulting product **4a**, whereas removal of

the sulfur ligand (**4a** → **3b**) is quite energy-demanding and accordingly associated with a significant shortening of the remaining Pt–N bond in the putative fragment **3b** to $r_{Pt-N} = 1.961$ Å. Likewise, the direct loss of the $(CH_3)_2S$ ligand (**1a** → **2a**) is associated with a significant shortening of the Pt–N bond in *trans* position to the sulfur ligand ($r_{Pt-N} = 1.980$ Å in **2a** compared to 2.084 Å in **1a**). The following loss of CH_4 (**2a** → **TS2a/2b** → **2b**) does not involve a Pt^{IV} intermediate and, when considering the fact that the position of the Pt–C bond changes with respect to the bisimino ligand, the bonding situation around Pt in **2b** is similar to that in **2a**, *i.e.*, $r_{Pt-C} = 2.030$ *vs.* 2.020 Å, a short (1.980 *vs.* 1.951 Å) and a long (2.165 *vs.* 2.163 Å) Pt–N bond with the latter *trans* to the Pt–C bond, and these features remain similar in the final product **3a**.

We are grateful to the *Deutsche Forschungsgemeinschaft (DFG)*, the *Fonds der Chemischen Industrie*, and the *Academy of Sciences of the Czech Republic* (Z40550506) for financial support. This project has also been funded by the *Cluster of Excellence 'Unifying Concepts in Catalysis'* coordinated by the *Technische Universität Berlin* and funded by the *DFG*.

REFERENCES

[1] A. E. Shilov, 'Activation of saturated hydrocarbons by transition metal complexes', Reidel, Dordrecht, 1984.
[2] R. A. Periana, D. J. Taube, S. Gamble, H. Taube, T. Sato, H. Fuji, *Science* **1998**, *280*, 560; J. A. Labinger, *J. Mol. Catal.* **2004**, *220*, 27.
[3] J. A. Labinger, J. E. Bercaw, *Nature* **2002**, *417*, 507; b) M. Lersch, M. Tilset, *Chem. Rev.* **2005**, *105*, 2471.
[4] a) H. Schwarz, D. Schröder, *Pure Appl. Chem.* **2000**, *72*, 2319; b) M. Heiberg, O. Gropen, O. Swang, *Int. J. Quant. Chem.* **2003**, *92*, 391; c) H. Schwarz, *Angew. Chem., Int. Ed.* **2003**, *42*, 4442; d) D. K. Bohme, H. Schwarz, *Angew. Chem., Int. Ed.* **2005**, *44*, 2336; e) M.-E. Moret, P. Chen, *Organometallics* **2007**, *26*, 1523; f) M. Armélin, M. Schlangen, H. Schwarz, *Chem.–Eur. J.* **2008**, *14*, 5229.
[5] J. A. Labinger, J. E. Bercaw, M. Tilset, *Organometallics* **2006**, *25*, 805; G. Gerdes, P. Chen, *Organometallics* **2006**, *25*, 809.
[6] L. Johansson, M. Tilset, J. A. Labinger, J. E. Bercaw, *J. Am. Chem. Soc.* **2000**, *122*, 10846; G. Gerdes, P. Chen, *Organometallics* **2003**, *22*, 2217; L. A. Hammad, G. Gerdes, P. Chen, *Organometallics* **2005**, *24*, 1907.
[7] B. Butschke, M. Schlangen, H. Schwarz, D. Schröder, *Z. Naturforsch., B* **2007**, *62*, 309.
[8] C. Hinderling, D. A. Plattner, P. Chen, *Angew. Chem., Int. Ed.* **1997**, *36*, 243; C. Hinderling, D. Feichtinger, D. A. Plattner, P. Chen, *J. Am. Chem. Soc.* **1997**, *119*, 10793.
[9] D. Schröder, H. Schwarz, N. Aliaga-Alcade, F. Neese, *Eur. J. Inorg. Chem.* **2007**, 816.
[10] M. Schlangen, J. Neugebauer, M. Reiher, D. Schröder, J. P. Lopez, M. Haryono, F. W. Heinemann, A. Grohmann, H. Schwarz, *J. Am. Chem. Soc.* **2008**, *130*, 4285.
[11] J. B. Fenn, *Angew. Chem., Int. Ed.* **2003**, *42*, 3871.
[12] D. Schröder, T. Weiske, H. Schwarz, *Int. J. Mass Spectrom.* **2002**, *219*, 729; C. Trage, D. Schröder, H. Schwarz, *Chem.–Eur. J.* **2005**, *11*, 619.
[13] http://winter.group.shef.ac.uk/chemputer/.
[14] D. Schröder, H. Schwarz, *Can. J. Chem.* **2005**, *83*, 1936.
[15] C. Lee, W. Yang, R. G. Parr, *Phys. Rev. B* **1988**, *37*, 785; A. D. Becke, *J. Chem. Phys.* **1993**, *98*, 5648.
[16] Gaussian 03, Revision C.02, M. J. Frisch, G. W. Trucks, H. B. Schlegel, G. E. Scuseria, M. A. Robb, J. R. Cheeseman, J. A. Montgomery Jr., T. Vreven, K. N. Kudin, J. C. Burant, J. M. Millam, S. S. Iyengar, J. Tomasi, V. Barone, B. Mennucci, M. Cossi, G. Scalmani, N. Rega, G. A. Petersson, H. Nakatsuji, M. Hada, M. Ehara, K. Toyota, R. Fukuda, J. Hasegawa, M. Ishida, T. Nakajima, Y. Honda, O. Kitao, H. Nakai, M. Klene, X. Li, J. E. Knox, H. P. Hratchian, J. B. Cross, V. Bakken, C. Adamo, J. Jaramillo, R. Gomperts, R. E. Stratmann, O. Yazyev, A. J. Austin, R. Cammi, C. Pomelli,

J. W. Ochterski, P. Y. Ayala, K. Morokuma, G. A. Voth, P. Salvador, J. J. Dannenberg, V. G. Zakrzewski, S. Dapprich, A. D. Daniels, M. C. Strain, O. Farkas, D. K. Malick, A. D. Rabuck, K. Raghavachari, J. B. Foresman, J. V. Ortiz, Q. Cui, A. G. Baboul, S. Clifford, J. Cioslowski, B. B. Stefanov, G. Liu, A. Liashenko, P. Piskorz, I. Komaromi, R. L. Martin, D. J. Fox, T. Keith, M. A. Al-Laham, C. Y. Peng, A. Nanayakkara, M. Challacombe, P. M. W. Gill, B. Johnson, W. Chen, M. W. Wong, C. Gonzalez, J. A. Pople, *Gaussian, Inc.*, Wallingford CT, 2004.

[17] A. Schafer, C. Hubers, R. Ahlrichs, *J. Chem. Phys.* **1994**, *100*, 5829.

[18] K. A. Peterson, D. Figgen, M. Dolg, H. Stoll, *J. Chem. Phys.* **2007**, *126*, 124101, and refs. cit. therein.

[19] K. Fukui, *J. Phys. Chem.* **1970**, *74*, 4161; K. Fukui, *Acc. Chem. Res.* **1981**, *14*, 363; C. Gonzales, H. B. Schlegel, *J. Phys. Chem.* **1990**, *94*, 5523.

[20] N. B. Cech, C. G. Enke, *Mass Spectrom. Rev.* **2001**, *20*, 362.

[21] N. Tsierkezos, D. Schröder, H. Schwarz, *J. Phys. Chem. A* **2003**, *107*, 9575.

[22] D. Schröder, M. Engeser, M. Brönstrup, C. Daniel, J. Spandl, H. Hartl, *Int. J. Mass Spectrom.* **2003**, *228*, 743.

[23] C. Trage, M. Diefenbach, D. Schröder, H. Schwarz, *Chem.–Eur. J.* **2006**, *12*, 2454; D. Schröder, M. Engeser, H. Schwarz, E. C. E. Rosenthal, J. Döbler, J. Sauer, *Inorg. Chem.* **2006**, *45*, 6235; P. Grüne, C. Trage, D. Schröder, H. Schwarz, *Eur. J. Inorg. Chem.* **2006**, 4546; B. Jagoda-Cwiklik, P. Jungwirth, L. Rulíšek, P. Milko, J. Roithová, J. Lemaire, P. Maitre, J. M. Ortega, D. Schröder, *ChemPhysChem* **2007**, *8*, 1629; S. Rochut, J. Roithová, D. Schröder, F. R. Novara, H. Schwarz, *J. Am. Soc. Mass Spectrom.* **2008**, *19*, 121; P. Milko, J. Roithová, D. Schröder, J. Lemaire, H. Schwarz, M. C. Holthausen, *Chem.–Eur. J.* **2008**, *14*, 4318; F. R. Novara, P. Gruene, D. Schröder, H. Schwarz, *Chem.–Eur. J.* **2008**, *14*, 5957.

[24] J. Schwarz, D. Schröder, H. Schwarz, C. Heinemann, J. Hrušák, *Helv. Chim. Acta* **1996**, *79*, 1110.

[25] G. Czekay, K. Eller, D. Schröder, H. Schwarz, *Angew. Chem.* **1989**, *101*, 1306; *Angew. Chem., Int. Ed.* **1989**, *28*, 1277; D. Schröder, H. Schwarz, *J. Am. Chem. Soc.* **1990**, *112*, 5947; D. Schröder, J. Roithová, P. Gruene, H. Schwarz, H. Mayr, K. Koszinowski, *J. Phys. Chem. A* **2007**, *111*, 8925; B. Butschke, M. Schlangen, D. Schröder, H. Schwarz, *Int. J. Mass Spectrom.*, submitted.

[26] A. Marrone, N. Re, R. Romeo, *Organometallics* **2008**, *27*, 2215.

[27] Y. Zhao, D. G. Truhlar, *Acc. Chem. Res.* **2008**, *41*, 157.

Received July 31, 2008